



Contents lists available at ScienceDirect

## Biochimica et Biophysica Acta

journal homepage: [www.elsevier.com/locate/bbabio](http://www.elsevier.com/locate/bbabio)

## Redox changes accompanying inorganic carbon limitation in *Synechocystis* sp. PCC 6803<sup>☆</sup>

Steven C. Holland, Anthony D. Kappell, Robert L. Burnap<sup>\*</sup>

Department of Microbiology and Molecular Genetics, Oklahoma State University, Stillwater, OK 74078, USA

## ARTICLE INFO

## Article history:

Received 19 October 2014

Received in revised form 26 November 2014

Accepted 2 December 2014

Available online 6 December 2014

## Keywords:

Photosynthesis

Carbon concentrating mechanism

NADH-1

NADPH

Fluorescence

Cyanobacteria

## ABSTRACT

Inorganic carbon ( $C_i$ ) is the major sink for photosynthetic reductant in organisms capable of oxygenic photosynthesis. In the absence of abundant  $C_i$ , the cyanobacterium *Synechocystis* sp. strain PCC6803 expresses a high affinity  $C_i$  acquisition system, the  $CO_2$ -concentrating mechanisms (CCM), controlled by the transcriptional regulator CcmR and the metabolites NADP<sup>+</sup> and  $\alpha$ -ketoglutarate, which act as co-repressors of CcmR by modulating its DNA binding. The CCM thus responds to internal cellular redox changes during the transition from  $C_i$ -replete to  $C_i$ -limited conditions. However, the actual changes in the metabolic state of the NADPH/NADP<sup>+</sup> system that occur during the transition to  $C_i$ -limited conditions remain ill-defined. Analysis of changes in the redox state of cells experiencing  $C_i$  limitation reveals systematic changes associated with physiological adjustments and a trend towards the quinone and NADP pools becoming highly reduced. A rapid and persistent increase in  $F_0$  was observed in cells reaching the  $C_i$ -limited state, as was the induction of photoprotective fluorescence quenching. Systematic changes in the fluorescence induction transients were also observed. As with Chl fluorescence, a transient reduction of the NADPH pool ('M' peak), is assigned to State 2→State 1 transition associated with increased electron flow to NADP<sup>+</sup>. This was followed by a characteristic decline, which was abolished by  $C_i$  limitation or inhibition of the Calvin–Benson–Bassham (CBB) cycle and is thus assigned to the activation of the CBB cycle. The results are consistent with the proposed regulation of the CCM and provide new information on the nature of the Chl and NADPH fluorescence induction curves.

© 2014 Elsevier B.V. All rights reserved.

## 1. Introduction

Inorganic carbon ( $C_i$ ) is an essential and often limiting macronutrient for the growth of organisms performing oxygenic photosynthesis. It serves as the major sink of photosynthetic reductant via incorporation into sugar carbon skeletons of the reductive Calvin–Benson–Benson (CBB) cycle. Correspondingly,  $C_i$ -limitation may result in the accumulation of electrons in carrier pools leading to the production of damaging reactive oxygen intermediates as well as the loss of overall photosynthetic efficiency due to photorespiration. Photorespiration results from the competition between  $CO_2$  and  $O_2$  at the active site of ribulose biphosphate carboxylase-oxygenase (RuBisCO) with the former giving

the productive carboxylation reaction of ribulose biphosphate (RuBP) and the latter leading to the wasteful oxygenation of RuBP. Accordingly, low  $CO_2$  or high  $O_2$  concentrations favor the oxygenation reaction over the carboxylation reaction. In aquatic environments, the potential for  $C_i$  limitation is particularly acute due to the low solubility and diffusivity of dissolved  $C_i$ . To avoid this, cyanobacteria and algae have evolved a  $CO_2$ -concentrating mechanism (CCM). The CCM may have emerged in the progenitors of contemporary cyanobacteria as they adapted to cope with increased photorespiration and lower efficiency carbon fixation accompanying a drop in  $CO_2$  levels and a rise in  $O_2$  levels during the Phanerozoic eon about 350 million years ago [1, 2] or perhaps an earlier epoch [3]. These adaptations include transport mechanisms for the active uptake of  $C_i$  [reviewed in [4,5]] that work together within a micro-compartment, known as the carboxysome, to localize and increase the local concentration of  $CO_2$  around RuBisCO, thereby improving the efficiency of  $CO_2$  fixation [reviewed in [6]]. Such mechanisms are highly effective and result in the accumulation of  $C_i$  over 1000-fold within the cyanobacterial cell relative to its environment [7,8]. Recent biotechnological efforts now consider utilizing the cyanobacterial CCM components as a model and source of molecular components for improving plant productivity [5,9,10].

The existence of two distinct physiological states defined by different  $C_i$  affinities was identified in *Chlamydomonas* depending upon

**Abbreviations:** CBB, Calvin–Bassham–Benson cycle of photosynthetic carbon fixation;  $C_i$ , inorganic carbon, primarily  $[HCO_3^- + CO_2]$ ; CCM,  $CO_2$  concentrating mechanism; 2PG, initial product of photorespiration due to the oxygenation reaction of RuBP by RubisCO; RuBP, ribulose biphosphate;  $\alpha$ -KG,  $\alpha$ -ketoglutarate or 2-oxoglutarate; RubisCO, ribulose biphosphate carboxylase/oxygenase; PSET, photosynthetic electron transport; LEF, linear electron flow; CEF, cyclic electron flow; GLY, glyceraldehyde; PQ, plastoquinone

<sup>☆</sup> This work was supported by the U.S. Department of Energy Basic Energy Sciences; grant no. DE-FG02-08ER15968.

<sup>\*</sup> Corresponding author at: Oklahoma State University, 307 Life Science East, Stillwater, OK 74078, USA. Tel.: +1 405 744 7445.

E-mail addresses: [rob.burnap@okstate.edu](mailto:rob.burnap@okstate.edu), [Robert.burnap@okstate.edu](mailto:Robert.burnap@okstate.edu) (R.L. Burnap).

whether cells were grown in air or CO<sub>2</sub>-enriched air [11]. Studies with cyanobacteria revealed that they also exhibit an inducible high affinity CCM [8,12]. The cyanobacterium *Synechocystis* sp. PCC 6803 (hereafter *Synechocystis*) exhibits a basal, lower affinity CCM when grown under C<sub>i</sub> sufficient conditions (e.g. gassing with air enriched with 3% v/v air, high C<sub>i</sub>, HC) and this depends upon low affinity C<sub>i</sub> transporters that are constitutively expressed [13,14]. The constitutively expressed low affinity uptake mechanism is comprised of multiple transporters, including Na<sup>+</sup>/HCO<sub>3</sub><sup>-</sup> symporters and a redox powered CO<sub>2</sub>-hydration enzyme, CupB (ChpX) that couples to the NADPH dehydrogenase complex (NDH-1) that collectively elevate the cytoplasmic concentration of HCO<sub>3</sub><sup>-</sup>. This form of the NDH-1 complex is denoted NDH-1<sub>4</sub> in reference to the alternative pair of intrinsic membrane protein D4/F4 subunits that are postulated to be involved in proton pumping based on homology with known structures [15] and bind the CupB (ChpY) protein [16]. Exposure of *Synechocystis*, and many other cyanobacterial species, to C<sub>i</sub>-limited growth conditions elicits the expression of a supplementary high affinity system. Under limiting C<sub>i</sub> conditions (bubbling with ambient air, low C<sub>i</sub>, LC) there is an induced increase in affinity for C<sub>i</sub> achieved through transcriptional up-regulation of transport activities and carboxysome components and, possibly, kinetic modification of existing transporters accounting for the higher affinity physiological state mentioned above. Alternative high affinity suites of proteins, including high affinity Na<sup>+</sup>/HCO<sub>3</sub><sup>-</sup> symporters and the high affinity CO<sub>2</sub>-hydration enzymes, are expressed when cyanobacteria are grown under C<sub>i</sub>-limiting conditions. The increase in transporter affinity for C<sub>i</sub> during limiting conditions is due to the transcriptional induction of the genes encoding the ATP dependent BCT1 high affinity HCO<sub>3</sub><sup>-</sup> transporter encoded by the *cmp* operon, Na<sup>+</sup>-dependent SbtA HCO<sub>3</sub><sup>-</sup> symporter, and the specialized NADPH dehydrogenase complex NDH-1<sub>3</sub> high affinity CO<sub>2</sub>-hydrating system encoded by the *ndhF3/ndhD3/cupA/cupS* operon. The NDH-1<sub>3</sub> complex is similar to the NDH-1<sub>4</sub> complex except that three specialized membrane intrinsic subunits, D4/F4/CupB, are replaced by their high affinity paralogs, the D3/F3/CupA subunits. The transcriptional regulation of the inducible transporters is controlled by the two self-regulating LysR-type transcriptional regulators known as CcmR (NdhR) [17–19] and CmpR [20,21]. The signal for induction of the transporter encoded by the *cmp* operon through CmpR has been identified as the co-activators ribulose-bisphosphate (RuBP) and 2-phosphoglycolate (2PG) [20]. The signals for the repression of the putative CcmR regulon controlling the expression of the *sbtA* gene, *ndhF3* operon, and the expression of a putative NDH-1 dependent Na<sup>+</sup> transporter are the co-repressors, α-ketoglutarate (α-KG) and oxidized nicotinamide adenine dinucleotide (NADP<sup>+</sup>) [19]. Thus, the internal metabolic state provides the regulatory cues for expressing the high-affinity system rather than inorganic carbon species per se.

The aim of the present study is to understand physiological changes that accompany, and potentially trigger, changes in the regulation CCM genes and to provide additional physiological context for previous experiments [13,18,22–25]. Because of the central role of NADPH in metabolism and because it acts as a critical signaling molecule in the regulation of the CCM, it is important to understand the dynamics of the redox state of the cellular pool of NADPH/NADP<sup>+</sup> in response to changes in the availability of C<sub>i</sub>. Previous studies have shown that the NADP pool is more reduced in cells grown in low-carbon conditions than those grown in under high-carbon conditions [26]. However, the physiological basis for this change is not fully understood. Furthermore, it is important to understand the dynamic properties of the redox state of NADP under fluctuating environmental conditions due to its role in regulating cellular processes. Blue green fluorescence has been developed as an approach to monitor changes in the redox state of the pyridine nucleotide pools in isolated intact chloroplasts and leaf fragments [27,28]. Similarly, the dynamics of redox changes in pyridine pools in cyanobacteria has yielded information on the role of NADPH in cyclic electron flow (CEF) [29]. The commercial availability of a DUAL-PAM-100 (Walz, Germany) allows for the simultaneous measurement of

chlorophyll a and NADPH fluorescence [30], which permitted the simultaneous *in vivo* investigation of the photosynthetic reducing equivalents of plastoquinone (PQ) and NAD(P)H. A recent investigation of *Synechocystis* NADPH transients has provided important insights into the quantitative use of this instrument and how the levels of NADPH fluctuate in response to different light regimes [31]. Importantly, that study also revealed, for the first time, the extent and kinetic properties to the electron transfers occurring from PSI to NADPH via ferredoxin NADP reductase (FNR).

This study aims to use these techniques in order to investigate cellular response to nutrient limitation (i.e. high and low carbon availability). Simultaneous chlorophyll and NADPH fluorescence provides insight into the relationship between the redox state of the PSET chain and its dependence on downstream metabolic processes, namely the CBB cycle.

## 2. Methods

### 2.1. Cell cultures and growth conditions

Experiments sampled 800 mL cultures of wild-type *Synechocystis* sp. PCC 6803 that were grown under 3% CO<sub>2</sub> bubbling conditions in 1 L Roux bottles in a modified BG11 medium [32] as described previously [18]. Modified media was identical to standard BG11 except omitting Na<sub>2</sub>CO<sub>3</sub>, adding HEPES to a concentration of 40 mM, and adjusting the pH to 7.0 using KOH, rather than NaOH.

### 2.2. Fluorescence measurements probing cells during the transition to C<sub>i</sub>-limited growth

A 250 mL sample of 3% CO<sub>2</sub> grown cells was centrifuged at 10,000 g for 5 min. Cells were gently re-suspended in fresh, CO<sub>2</sub> bubbled, low-C<sub>i</sub> BG-11 media to a chlorophyll concentration of 5 µg/mL in a 2 mL sample. The sample was placed in a 10 mm open quartz cuvette with a small stir bar. Cells were exposed to red actinic light (~100 µE) and stirred for up to approximately 16 h. Stirring occurred at a pace that maintained cells in suspension, but did not cause excessive aeration of the sample and therefore inorganic carbon concentrations within the sample could not be replenished at a rate that can keep pace with consumption by cells in the sample performing photosynthesis. Accordingly, samples exhibited fluorescence characteristics of indicative of C<sub>i</sub>-limitation approximately 8 h into the experiment.

Every 15 min during the approximately 16 hour assay, the stirring and actinic light would be turned off. After 30 s of this dark acclimation period, a measuring trace would initiate recording the fluorescence yield from the measuring beam in the dark. Dark period fluorescence was measured for 1 min, with an intense 300 ms multiple turnover (MT) flash occurring at 35 s. At 60 s, the actinic light was turned on. The sample was exposed to actinic light for 270 s, with a MT flash occurring 250 s after the actinic light exposure. Post-illumination measurement continued for 80 s, with a MT flash occurring 70 s after stopping illumination. Nine seconds after the (MT), actinic light exposure and stirring resumed. As shown in Supplemental Fig. S1, growth of cells was maintained although gradual and in a manner consistent with previous observations in normal growth bottles used for gene expression experiments [18]. The parameters of Chl fluorescence characterizing the induction curves follow the calculation and nomenclature described by Campbell et al. [33].

## 3. Results and discussion

### 3.1. PAM fluorescence measurements of redox changes in cells during C<sub>i</sub>-limitation

To investigate the changes in the cellular redox state in response to C<sub>i</sub>-limitation, pulse-amplitude modulated (PAM) fluorometry was utilized (Fig. 1). Chlorophyll fluorescence is widely used for the analysis

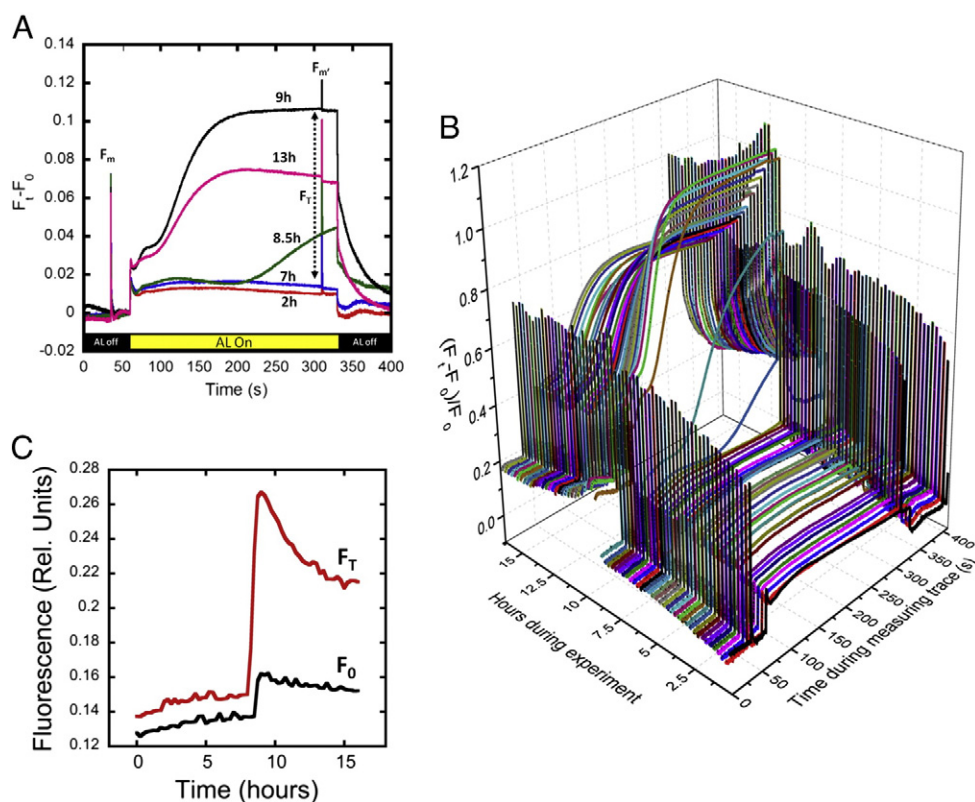


**Fig. 1.** Changes in the Chl induction kinetics during the course of inorganic carbon limitation of *Synechocystis* cells. Panel A: Chlorophyll fluorescence traces of cells switched from bubbling with 3% CO<sub>2</sub> enriched air to stirring under illumination in a 10 mm cuvette of a sample undergoing C<sub>i</sub> depletion in a PAM fluorometer. Cells were illuminated with actinic red illumination at 110 μE except during the intermittent dark periods at the beginning and end of the actinic light periods of data acquisition. Selected chlorophyll fluorescence induction curves at the time points of 2 (red), 7 (blue), 8.5 (green), 9 (black), and 13 (pink) hours after changing the C<sub>i</sub> conditions. After a 60 second dark adaptation (first repetitive intermittent dark period, black bar), actinic light was turned on at 60 s (yellow bar) and turned off at 330 s for the post-actinic illumination portion of the data collection trace (second repetitive intermittent dark period, second black bar). Multiple turnover flashes were performed during the dark interval and actinic illumination periods at the 30 and 310 time points in the trace (F<sub>m</sub> and F<sub>m</sub>′, respectively). Panel B: Overall perspective showing all chlorophyll fluorescence transients during the C<sub>i</sub>-deprivation experiment. Panel C: Changes in F<sub>0</sub> and F<sub>T</sub> during the course of the C<sub>i</sub> deprivation. Black line: F<sub>0</sub>, chlorophyll fluorescence value 1 s before actinic illumination; Red line: F<sub>T</sub>, steady state fluorescence during actinic illumination defined at the 300 sec time point.

of both linear electron flow (LEF) and cyclic electron flow (CEF) and thus the PAM technique provides information on basic photosynthetic parameters. The use of PAM fluorometry to track changes in the redox state of NAD(P)H as blue-green fluorescence is not as widely used, but the technique has the potential to uncover possible redox transients in vivo with high time resolution [27,28,30] as realized in recently reported work [31]. Because NADPH and NADH possess virtually identical fluorescence characteristics, it is impossible to distinguish which species is responsible for the fluorescence transients, and though physiological investigations have indicated that the transients observed under light changes are largely due to NADPH [29], this limitation remains. Simultaneous monitoring of chlorophyll and NAD(P)H fluorescence of samples was performed in a PAM-100 device (Walz) and a HC→LC downshift routine was developed to roughly emulate the C<sub>i</sub>-downshift conditions used previously [18]. For PAM fluorometry, small samples (2 mL) of culture were maintained directly in the optical cuvette and allowed to deplete the media of C<sub>i</sub> under illumination with red LEDs and stirring. Another difficulty lies in potential cell growth during the assay. The cells appear to behave in a manner consistent with earlier transcriptional profiling experiments [18], with growth becoming negligible after carbon depletion (Fig. S1). Thus, it appears that the application of the biophysical techniques described below should be a reasonable approximation to the experimental conditions utilized earlier for the gentle C<sub>i</sub> downshift experiment global gene expression profiling and therefore it should be possible to connect the biophysical changes with those of the transcriptional changes.

Fig. 1A shows selected chlorophyll fluorescence induction traces at different stages of C<sub>i</sub>-limitation. Early in the experiment, while the cells have sufficient C<sub>i</sub>, the briefly dark-adapted cells exhibit a

characteristic fluorescence induction profile when actinic illumination is resumed. Actinic light powers photosynthetic electron transport, resulting in an increase in chlorophyll fluorescence, indicative of an increase in the number of ‘closed’ PSII reaction centers, corresponding to an increase in the concentration of reduced acceptor, Q<sub>A</sub><sup>-</sup> and, correspondingly, a higher yield of chlorophyll fluorescence [33]. This reflects a quasi-steady state balance of rates corresponding to the actinic excitation rate generating Q<sub>A</sub><sup>-</sup> (Q<sub>A</sub> reduction rate) and the rate of forward electron transfer of electron into the PQ pool via the PSII Q<sub>B</sub> site (Q<sub>A</sub><sup>-</sup> oxidation rate). CBB cycle activation, state transitions, and other bioenergetic and metabolic processes influence their rates and result in additional transients that eventually dampen to a steady state fluorescence level that is maintained throughout the remainder of the actinic illumination period.

Early in the C<sub>i</sub>-deprivation experiment, upon illumination of briefly dark adapted cells, a steady state fluorescence level is reached after ~20 s of actinic illumination (~80 sec point on the trace) and remains low compared to maximal fluorescence (denoted F<sub>m</sub>′) in the C<sub>i</sub>-replete cells shown as the red trace in Fig. 2A. This corresponds to a largely oxidized PQ pool under these illumination conditions, which were designed to approximate the growth light intensities. Correspondingly, this allows the efficient re-oxidization Q<sub>A</sub><sup>-</sup>, thereby maintaining, on balance, about 85% of PSII centers in the open condition (i.e. photochemical quenching, q<sub>p</sub> ~ 0.85). This situation changes dramatically as discussed below, when the cells proceed into the C<sub>i</sub>-limited state, where PSII is found mostly in the closed state under actinic illumination. Saturating multiple turnover flashes were given, one during the dark adaptation (F<sub>m</sub>) and one toward the end of the actinic illumination period (F<sub>m</sub>′), with the latter having a considerably larger amplitude.

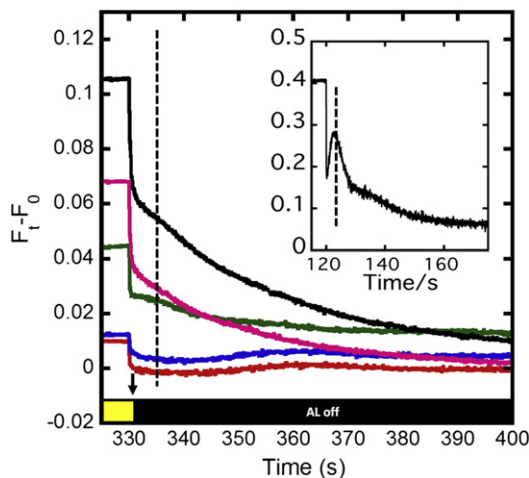


**Fig. 2.** Post-actinic illumination fluorescence transients during the course of inorganic carbon limitation of *Synechocystis* cells. Selected chlorophyll fluorescence post-illumination transients at the time points of 2 (red), 7 (blue), 8.5 (green), 9 (black), and 13 (pink) hours after changing the  $C_i$  conditions. Post-illumination Chl fluorescence transients show that  $C_i$ -limitation enhances the peak occurring  $\sim 5$  s after the cessation of actinic illumination (vertical dotted line). This peak in Chl fluorescence is attributed to cyclic electron transfer [29,46,48,49]. Inset: Post-illumination Chl fluorescence peak is most readily observed with shorter actinic illumination periods and in cells grown under low  $C_i$  conditions (BG-11 media, slow air bubbling, pH 7), which induces the high affinity CCM including NDH-1<sub>3</sub>.

This indicates that the cells are undergoing state transitions during the light–dark cycling with cells reaching the State 2 condition in the dark period and then reverting back to State 1 in the light. State 2 corresponds to the molecular configuration where excitation energy from the phycobilisome is increasingly directed to PSI, which is a more efficient quencher of excitation energy than PSII. Resumption of actinic illumination drives the State 2→State 1 transition resulting in more excitation energy from the phycobilisome being directed to PSII providing the higher fluorescence yields seen with the second saturating flash,  $F_m'$  (Fig. 1A). Recent work has assigned the slow S–M fluorescence rise occurring during the first 20 s after application of actinic illumination rise to the State 2→State 1 transition [34]. This assignment is consistent with our experiments where an additional MT flash is given 25 s after the re-initiation of actinic illumination (at the 85 sec time point), where it was observed that the higher yield of fluorescence is already elicited indicating that State 2→State 1 transition has already occurred at the end of the S–M phase of the induction curve (Supplemental Fig. S3).

As the availability of  $C_i$  decreases later in the experiment (Fig. 1, hours 8.25 and after), the characteristic fluorescence induction profile begins to exhibit a new secondary rise phase in the fluorescence yield (Fig. 1A). This secondary phase first appears late in the actinic illumination period, but as the cells become progressively more  $C_i$ -limited, the secondary rise phase is observed earlier and earlier in the actinic illumination portion of the measuring trace (Fig. 1A, green, black, and pink traces). At the 9 hour trace (Fig. 1A, black trace), the increase in fluorescence yield begins within 25 s of switching on actinic illumination and its level soon approaches maximal fluorescence ( $F_m'$ ), indicating nearly complete closure of all PSII reaction centers under actinic illumination. Thus, upon reaching the fully  $C_i$ -limited condition, virtually all PSII centers are in the closed state (mostly  $Q_A^-$ ) as the availability of PSII electron acceptor vanishes with all the PQ pool having been converted to the reduced form. This is reflected in the decrease in the re-oxidation rates deduced from the post-actinic illumination fluorescence decays as discussed in the next section. It is also consistent with observations that maximal chlorophyll fluorescence occurs in cyanobacterial cells when they reach the  $CO_2$  compensation point [35–37]. This over-reduced condition is due to  $C_i$ -limitation, since the addition of bicarbonate to the cells in the sample cuvette restores the lower fluorescence

and kinetic features observed early in the experiment (Supplemental Fig. S2) [36,38–41]. We conclude that as  $C_i$  limitation becomes progressively more severe, the second rise phase commences progressively earlier as a consequence of an increasingly smaller pool of oxidized CBB cycle intermediates, the major sink of photosynthetic reductant, consistent with earlier observations [35–37].

Fig. 1B illustrates the overall experiment, allowing the visualization of these and other trends in the form of a 3D plot that stacks the individual Chl fluorescence measuring traces collected over the entire course of the  $C_i$ -limitation experiment. It can be seen that the transition from the low fluorescent to high fluorescent state occurs within a period of about 30 min starting at the 8.25 hour time point. It is also clear that upon reaching the  $C_i$ -limited state, protective mechanisms involving the induction of some form of non-photochemical quenching ( $q_N$ ) are elicited. This is evidenced by the decrease in maximal fluorescence starting after 8.25 h (compare magnitude of fluorescence at 9 h, black trace versus the lower level at 13 h in Fig. 2A). This is more clearly seen in a plot of  $F_T$ , the steady state level of fluorescence under actinic illumination (Fig. 1C, red trace). Here,  $F_T$  is defined as the level of fluorescence at the 300 second point in the overall trace as indicated by the vertical dotted line in Fig. 1A.  $F_T$  reaches a maximum approaching that of maximal fluorescence ( $F_m'$ ), indicating most PSII centers are closed due to the absence of oxidized acceptor in the over-reduced PQ pool as the lack of available  $C_i$  reaches a critical point. However, after reaching this maximum, there is then a steady decline of  $F_T$  as protective non-photochemical ( $q_N$ ) processes are mobilized (Fig. 1C, red trace). This likely reflects increased activity of photoprotective processes including the action of the flavodiiron proteins, which are associated with the phycobilisome and are proposed to dissipate excess reductant from NADPH and PSII [35,42–44]. On the other hand, the orange carotenoprotein (OCP), involved in dissipative phycobilisome fluorescence quenching, is not likely involved since red light served as the actinic source and blue-green light activates OCP [45]. This is one possible mechanism for the observed induction of photochemical quenching. Nevertheless, other alternatives also not depending upon OCP cannot be yet excluded as an explanation for the strong gradual decline in maximal fluorescence after cells reach the  $C_i$ -limited state. For example, the dissipation of reductant via the induction of the NDH complexes associated with the CCM may contribute to the quenching [46].

Another redox feature associated the transition to the  $C_i$ -limited physiological state is the occurrence of a sharp increase in  $F_0$  seen beginning at the 8.25 hours trace (Fig. 1C, black trace). This increase in  $F_0$  is not reversed by the addition of bicarbonate (Fig. S2). Because the post-illumination decay occurs more slowly in  $C_i$ -limited cells (Fig. 2), there existed a possibility that the higher  $F_0$  occurred as a consequence of the slow decay of  $F_0$  due to the absence readily available oxidized carriers and processes that donate electrons to the PQ pool during the dark adaption phase of the light dark cycle. To test this, the dark acclimation interval between measuring traces was increased from 30 to 120 s, yet the fluorescence still decayed asymptotically to the higher  $F_0$  position (not shown), indicating the new higher level of  $F_0$  induced by the  $C_i$  deprivation corresponds to a relatively long-lived physiological state. Additionally, the higher  $F_0$  does not appear to be due to a state transition since these are observed to occur in a cyclic fashion, as noted above, and the higher  $F_0$  due to  $C_i$  depletion persists during the light–dark cycles of the experimental regime. Thus, the origin of the sharp increase in  $F_0$  remains unresolved. It could be speculated that the higher  $F_0$  might be a result of uncoupling of part of the phycobilisome antennae (e.g. partial disassembly of rods) in a process distinct from state transitions. Alternatively, it could relate to increase redox state of the PQ pool from increased activity of cyclic electron flow or by increased flow through the oxidative pentose phosphate pathway, as sugars are being consumed to compensate for carbon limitation. These alternatives remain hypothetical, yet the phenomenon of increased  $F_0$  does appear to be a novel finding regarding the process of adaptation to nutrient deprivation.

### 3.2. Post-illumination chlorophyll fluorescence kinetics

When the actinic illumination light is switched off, the decline in fluorescence is not monotonic, but exhibits fluctuations during the return to the  $F_0$  level (Fig. 2). As shown previously, these post-illumination fluctuations in the PQ pool redox state are strongly influenced by CEF and the flow of reductant to the membranes from oxidative metabolism (e.g. pentose phosphate pathway) [29,46–49]. Upon termination of the actinic light (Fig. 2, downward arrow, 330 s), fluorescence drops as reaction centers open due to re-oxidation of  $Q_A^-$  by electron transfer to PQ in the  $Q_B$  site. The exchange into and out of the  $Q_B$  site occurs in the ~5 millisecond time range, which is too fast for the time resolution of these measurements, where the data was collected at a rate of 1 point/ms and with noise levels of about 20% of this comparatively small decaying signal (~15%  $F_m$ ). However, this poorly resolved fast phase was gradually accompanied by the development of slower phases (Figs. 2 and S5) during the course of depletion. The decay of accumulated  $Q_A^-$  became multiphasic: the fast fluorescence decay phase ( $t_{1/2} \sim 5$  ms) remained about the same relative amplitude as before, but the descent was from the much higher fluorescence level ( $F_T$ ) of the  $C_i$ -starved state and dominated by slower decay processes. Two new decay phases with half times of ~240 ms and ~29 s, comprise about 30% and 60%, respectively of the total decline from  $F_T$  from cells in the  $C_i$ -depleted state (Table S1 and Fig. S5). These rate constants are only considered as apparent rates due to the presumed complexity of the underlying redox mechanisms, which may include a rate limitation of oxidation of the PQ pool by  $O_2$ -dependent oxidases [50]. Nevertheless, the net effect is that the slowdown of  $Q_A^-$  oxidation accounts for the accumulation of  $Q_A^-$  and the high  $F_T$  from cells in the  $C_i$ -depleted state as the CBB cycle becomes a less efficient sink for electrons.

During the first 10 s of the post-illumination period there is a kinetic 'shoulder' in the decline of fluorescence, depending on  $C_i$  availability (Fig. 2, inset). This dark increase in fluorescence has been attributed to CEF, predominantly through NDH-1 complexes [29,46,48,49,51]. Under the current experimental conditions, this peak is not observable early in the experiment (undetectable in the red and blue traces of Fig. 2). However, as  $C_i$ -limiting conditions prevail later in the experiment, it is possible to observe this increase (Fig. 2, green and black traces, indicated with a vertical dotted line). This shoulder becomes apparent at ~5 s after actinic light is switched off (Fig. 2, denoted with the vertical dotted line). This kinetic feature becomes more pronounced as CEF fluxes increase under conditions where the expression of NDH-1<sub>3</sub> complexes is maximized (i.e. growing cells under LC conditions for several days). This is illustrated in the inset of Fig. 2, showing the corresponding trace obtained from *Synechocystis* cells grown under LC conditions and giving results very similar to recent experiments [46,49]. Note the increase in fluorescence ~5 s after actinic light is switched off, denoted vertical dotted line in the inset of Fig. 2. In contrast, the present experimental cultures were grown under  $C_i$ -replete conditions and switched to  $C_i$ -limiting conditions. Because we have not measured the expression of the NDH-1<sub>3</sub> complexes [see e.g. [24]], it is not possible to determine whether the observed shoulder is due to NDH-1<sub>3</sub> complexes or whether other routes of CEF account for the peak [51]. However, it does seem likely that NDH-1<sub>3</sub> complexes are beginning to be expressed and accumulated as  $C_i$  becomes limiting given the similarity to previous experiments [18,24]. As the cells become more thoroughly  $C_i$ -limited and as PQ pool becomes more reduced, the post-illumination shoulder is obscured by the very slow decay phase in the decline of fluorescence yield discussed above (Fig. 2, pink trace). Besides the 5–10 s post-illumination peak and the slow decay features that increase with  $C_i$ -deprivation, it is also interesting to notice an additional kinetic feature: a low amplitude and broad fluorescence increase, that occurs approximately 35 s after the actinic light is switched off. This roughly corresponds to a similar feature seen in the NADPH post-illumination traces (Fig. 3B) and probably corresponds to an influx of metabolic reductant into the PQ pool

from oxidative carbon metabolism in the cytoplasm as discussed below.

### 3.3. Spectroscopic probes of NADPH during $C_i$ -limitation

Blue-green fluorescence has been used as a tool to analyze NADPH levels in vivo [27–29,31]. Changes in blue-green fluorescence could potentially be due to NADH fluorescence also occurring at these wavelengths. However, Mi et al. (2000) noted in *Synechocystis* that short-term changes in fluorescence during actinic illumination were eliminated with treatment of DCMU and DBMIB consistent with the main contribution to the transients as being that from NADPH. Recently, the increase in blue-green fluorescence due to single turnover flashes was best explained by the transfer of electrons from PSI to NADPH via FNR [31]. As shown in Fig. 3, the shape of the transients produced by actinic illumination during the  $C_i$ -limitation experiment shows several similar features with the Chl fluorescence transients acquired in parallel. As with the Chl fluorescence induction profile, blue-green fluorescence quickly rises upon the resumption of actinic illumination (Fig. 3A, 60 second time point) and is followed by multiphasic modulations in amplitude that reflect multiple cellular processes that affect the redox state of the NAD(P)H pool. During the first 30 s of actinic light exposure, similar multiphasic changes are observed over all periods of carbon availability. For all traces during the experiment, an initial rise occurs quickly due to PSI reduction of  $NADP^+$ , falls slightly during the ensuing ~8 s, and then rises again to a maximal point, labeled ' $N_M$ ' in Fig. 3A. This secondary rise,  $N_M$ , peaks ~25–30 s after the initial fast rise initiated by resumption of actinic illumination. Similar kinetic features are observed for Chl fluorescence induction kinetics, and there is solid evidence that the corresponding secondary rise to what is referred to as the 'M' peak, corresponds to the State 2 → State 1 transition in cyanobacteria [34]. Moreover, the Chl fluorescence experiment described above, where a measuring flash was inserted at the M peak, also provide evidence for this assignment. The State 2 → State 1 transition is the adjustable light-harvesting configuration where excitation energy is increasingly directed to PSII at the expense of PSI excitation. Correspondingly, the increased excitation of PSII with cells in State 1 will tend to maximize the rate of whole chain LEF further increasing the level of NADPH in the process. The assignment of the secondary NADPH increase (the  $N_S$  to  $N_M$  rise) to an increased rate of LEF due to the State 2 → State 1 transition, which is consistent with the observation that this secondary peak lags the Chl fluorescence M peak by several seconds, as might be expected from the proposed causal sequence with NADPH redox kinetics lagging behind PQ redox kinetics. Therefore, the rise in NAD(P)H fluorescence to the  $N_M$  peak is likely a consequence of the excitation energy redistribution of the State 2 → State 1 transition.

After ~25 s of actinic light exposure (Fig. 3A), striking differences between NAD(P)H fluorescence traces from  $C_i$ -replete and  $C_i$ -limited cells are observed. Before the onset of carbon limitation, a pronounced drop in reduced NADPH is observed after reaching the maximum,  $N_M$  (Fig. 3A). This re-oxidation of the NAD(P)H pool after  $N_M$  may be attributed to activation of the CBB cycle by analogy with suggestions from Chl fluorescence transients [52]. This decline in NAD(P)H fluorescence proceeds for approximately 60 s before reaching a new lower steady state level under the  $C_i$ -replete conditions. Presumably, the new lower level corresponds to a balance in rates of production of NADPH by LEF and the rate of consumption by  $CO_2$  fixation in the fully activated CBB cycle. Provided that the resultant sugars also have a sufficient utilization sink, this steady-state level of NADPH would continue without further modulations. Support for this assignment comes from the observation that as cells become increasingly  $C_i$ -starved, this decline disappears and instead, the steady state level of NAD(P)H fluorescence remains at a high value close to the  $N_M$  peak (Fig. 4A, 7 h and later traces). This is likely due to a hindered CBB cycle resulting in less NADPH being oxidized. This assignment is also supported by the observation that the addition of the CBB cycle inhibitor GLY abolishes this decline after

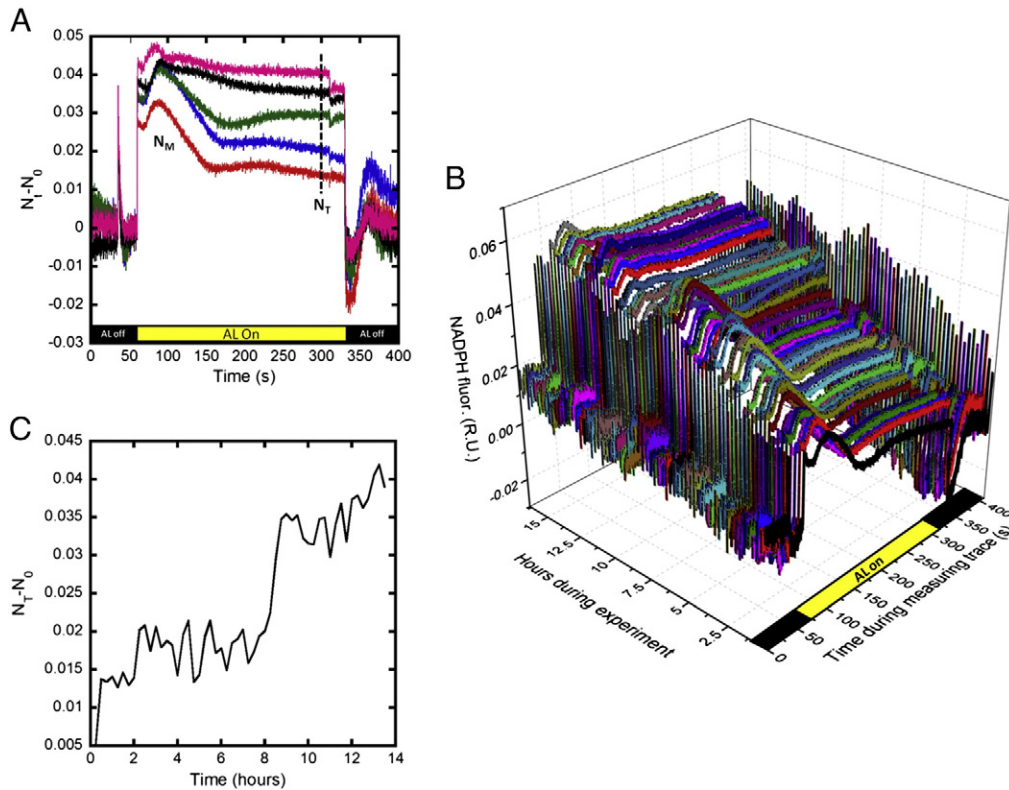


**Fig. 3.** Changes in the NAD(P)H kinetics during the course of inorganic carbon limitation of *Synechocystis* cells. Panel A: Selected NAD(P)H fluorescence traces of cells switched from bubbling with 3% CO<sub>2</sub> enriched air to stirring under illumination in a 10 mm cuvette of a sample undergoing C<sub>i</sub> depletion in a PAM fluorometer. Cells were illuminated with actinic red illumination at ~100 μE except during the intermittent dark periods at the beginning and end of the actinic light periods of data acquisition. After a 60 s dark adaptation (first repetitive intermittent dark period, black bar), actinic light was turned on at 60 s (yellow bar) and turned off at 330 s for the post-actinic illumination portion of the data collection trace (second repetitive intermittent dark period, second black bar). The selected traces are for the time points at 2 (red), 7 (blue), 8.5 (green), 9 (black), and 13 (pink) hours after changing the C<sub>i</sub> conditions. N<sub>M</sub> represents the maximum occurring after resumption of actinic illumination by analogy with 'M' of the Chl fluorescence induction nomenclature (see text). Panel B: Overall perspective of NAD(P)H fluorescence transients of a cell sample exposed to C<sub>i</sub> limitation. Panel C: Changes in N<sub>T</sub> during the course of the C<sub>i</sub> deprivation, N<sub>T</sub> is here defined as the terminal steady state NAD(P)H fluorescence during actinic illumination, sampled at the 300 sec time point (vertical dotted line).

the N<sub>M</sub> peak (Fig. 5). The limitation in available oxidizers of NADPH is reflected in the parameter N<sub>T</sub>, defined as the steady state NAD(P)H fluorescence during actinic illumination defined at the 300 sec time point (Fig. 4A, vertical dotted line). This limitation is illustrated in the plot of N<sub>T</sub> as a function of the time during the C<sub>i</sub>-deprivation experiment

shown in Fig. 3C. From these data, it can be inferred that illuminated cells have a more reduced NADPH pool in steady-state in C<sub>i</sub>-limited conditions, as opposed to those in C<sub>i</sub>-replete. Due to the duration of the experiment and uncertainty due to instrument drift, it is difficult to distinguish between the increase in N<sub>0</sub> due to cell growth and that

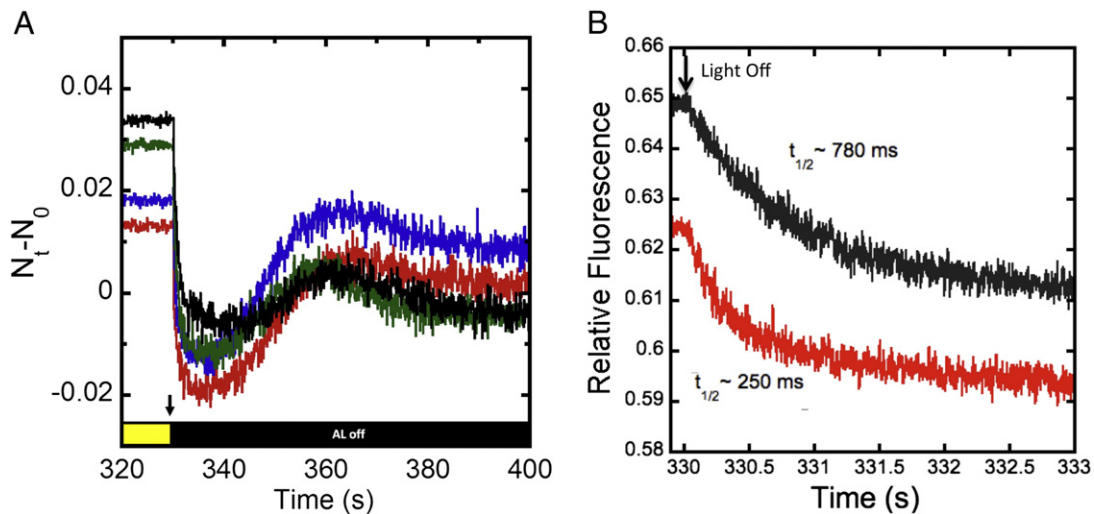


**Fig. 4.** Post-illumination changes in NAD(P)H fluorescence. Panel A: Selected NAD(P)H fluorescence post-illumination transients at the time points of 2 (red), 7 (blue), 8.5 (green), and 9 (black) hours after changing the C<sub>i</sub> conditions. Post-illumination NAD(P)H fluorescence transients exhibit a characteristic oxidation phase followed a re-reduction phase peaking at about 30 s after the cessation of the actinic light is switched off at 330 s. Panel B: Averaged post-illumination decays of NAD(P)H fluorescence during the first three seconds following termination of actinic illumination: Average of 20 traces prior to C<sub>i</sub>-depletion (red) and 20 traces after C<sub>i</sub>-depletion (black). Downward arrows indicate termination of actinic illumination.

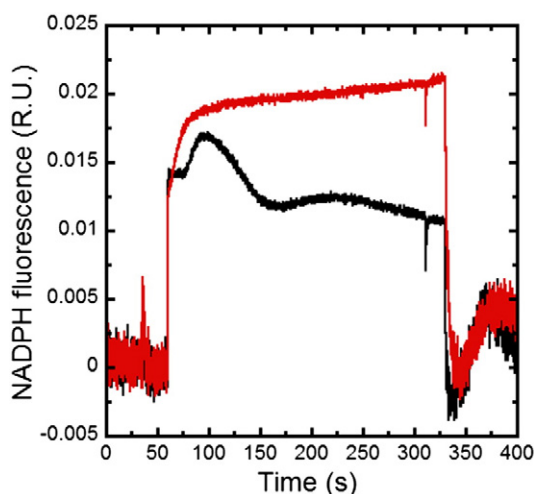


**Fig. 5.** The effect of Calvin–Benson–Basham cycle inhibitor glycolaldehyde on NADPH fluorescence induction. NADPH fluorescence transients of a HC cell culture before (black trace) and after (red trace) the addition of 10 mM glycolaldehyde. Cells re-suspended at a concentration of 5  $\mu\text{g}$  Chl mL. Periods of illumination are similar to those previously described except the cells were dark adapted 30 min and only 5 cycles of illumination were given and the five traces for each treatment were averaged.

due to a change in redox state, yet from the data presented here, and data from previous biochemical studies [26,53], it can be seen that there is an overall increase in the reduction state of the NAD(P)H pool during the course of depletion. This jump in the level of  $N_T$  also appears to slightly precede the sharp jump in  $F_0$  and  $F_T$  also observed during the course of  $C_i$ -limitation (Fig. 1C versus Fig. 3C). So in this case, the change in NADPH redox state precedes the changes in PQ redox state, as might be expected since the accumulation of reductant in the NADP pool occurs first following the onset of  $C_i$ -limitation and the effect propagates backwards and slows the flow of electrons in the electron transport chain as PSI acceptor becomes more sparse.

#### 3.4. Post-illumination NAD(P)H fluorescence transients

Post-illumination transients in NAD(P)H fluorescence also reveal interesting differences as cells become increasingly  $C_i$ -starved (Fig. 4). After turning off the actinic light (downward arrows), there is a sharp decline in blue-green fluorescence as LEF ceases to drive electrons into the NADPH pool, yet NADPH consumption pathways remain in their active light-adapted state resulting in an undershoot as previously observed [29–31]. These results show that in  $C_i$  replete conditions, the NAD(P)H fluorescence decline is rapid ( $t_{1/2} \sim 250$  ms) indicative of the avidity and high absorptive capacity of these NADPH-utilizing pathways. However, upon carbon limitation, the fluorescence half-time increases to  $\sim 780$  ms. From a practical perspective, the rapidity of these declines highlights the difficulty in performing rapid-quench biochemical analysis procedures to evaluate the redox state of the pyridine nucleotide pool.

Early in the experiment, the rapid post-illumination decline and ‘undershoot’ reaches its perigee  $\sim 6$  s after the cessation of actinic illumination followed by a biphasic return to the dark steady state level,  $N_0$ . In  $C_i$ -replete cells (Fig. 4, red traces), this biphasic return corresponds to a secondary rise peaking  $\sim 35$  s after the light is switched off. However, as cells proceed into the  $C_i$ -limited state, this secondary peak is diminished and shifted to earlier times (Fig. 4A, black trace). Additionally, the peak corresponds in time to a peak seen in post-illumination Chl fluorescence mentioned above (see also Supplementary Fig. S4). These peaks are tentatively assigned to the oxidation sugars accumulated in the cytoplasm during the light period which causes the reduction of the pyridine nucleotide pools with electrons transferred the PQ pool for oxidation in the thylakoid located respiratory pathway. As discussed,

during chlorophyll fluorescence, a reduction event associated with CEF mediated through NDH-1 complexes becomes more pronounced. Interestingly, very little change occurred within NADPH fluorescence the first 7 s after actinic light termination. While the amplitude of the decay increased, no new transient peaks or shoulders during the decline were observed. The absence of the corresponding feature in the NAD(P)H fluorescence decay occurring 7 s after actinic light termination is consistent with the oxidation of NADPH by both the CBB cycle as well as by the respiratory complexes NDH-1 complexes, with the latter contributing to the peak observed during the decay of Chl fluorescence (Fig. 2).

#### 4. Summary and conclusions

The analysis of changes in the redox state of *Synechocystis* cells experiencing  $C_i$  limitation reveals systematic kinetic changes and, as would be expected, a trend towards the quinone and pyridine nucleotide cofactor pools becoming highly reduced. With the ability to measure both chlorophyll and NADPH fluorescence simultaneously, a more complete model of fluorescence kinetics can be created (See Fig. 6). Changes in NADPH levels are likely to be the major contributor the blue green fluorescence transients observed in response to the changing light and nutrient availability, supporting earlier conclusions based upon inhibitor studies [29] and recent kinetic analyses [31]. Despite many years of observation, the underlying physiological bases for many of the undulations in the Chl fluorescence induction curves are not completely understood. Obviously much is known: starting with the observation that dark-adapted cells will have a basal chlorophyll fluorescence given by the parameter  $F_0$ , corresponding to maximal open PSII reaction centers and basal fluorescence due to the decay of excitons in proximal and distal light harvesting antennae, which escape being trapped at the reaction centers. The analogous parameter in NADPH fluorescence,  $N_0$ , corresponds to a dark-adapted level of NADPH, where cellular metabolism has reached steady state. Upon illumination, chlorophyll fluorescence undergoes a series of distinct modulations (OJDIIP rise, not illustrated in Fig. 6) before reaching a local peak,  $F_p$  within the first 2–3 s of illumination. These modulations correspond to intra-molecular electron transfer reactions within PSII but are affected by the rate of re-oxidation of  $Q_A^-$  by secondary acceptors [54]. NADPH fluorescence also responds to actinic illumination by reaching a local maximum,  $N_p$  in a similar time frame. It is likely that the kinetic similarities are due to the strong dependence of electron flow through PSI depending upon the flow through PSII with modulation by the state of the intersystem electron transport chain. Similarly, an inhibition of the major sink of photosynthetic electrons,  $\text{CO}_2$ -fixation via the CBB, results in the accumulation of electrons within the electron transport chain and the consequent diminished ability of the PQ pool to re-oxidize  $Q_A^-$ . This intimate connection between the PSII acceptor and the CBB cycle is observed as a larger  $F_p$  peak upon reaching the  $C_i$ -limited state (Fig. 1A) and in the presence of glycolaldehyde (not shown). After reaching the  $F_p$  peak, chlorophyll fluorescence drops to a local stationary state,  $F_s$ . The cause of this decline has been fully resolved [54], but NADPH fluorescence also reaches a local minimum/stationary phase at this time ( $N_s$ ). From this point, a rise in both chlorophyll and NADPH fluorescence is observed: for Chl fluorescence this is the  $F_s$  to  $F_M$  rise. This has been attributed to State 2  $\rightarrow$  State 1 transition in cyanobacteria [34]. The subsequent decline from  $F_M/N_M$  is not reversion of this state transition, but instead can be attributed to the activation of the CBB cycle, where in  $C_i$ -replete conditions NADPH is consumed, and in  $C_i$ -limited environments, both Chl and NADPH fluorescence remain high. Photochemical quenching through the activation CBB cycle permits a decline in chlorophyll fluorescence at  $F_M$  as regenerated  $\text{NADP}^+$  remains available as an electron sink. However, when the CBB cycle is impaired, a rise in both chlorophyll fluorescence and NADPH is observed and evolves to higher fluorescence levels ( $F_T$  and  $N_T$ ) upon reaching steady state, which requires about 2 min of actinic illumination in the present experiments (Figs. 1 and 2). As cells reach the  $C_i$ -limited state, a rapid and persistent

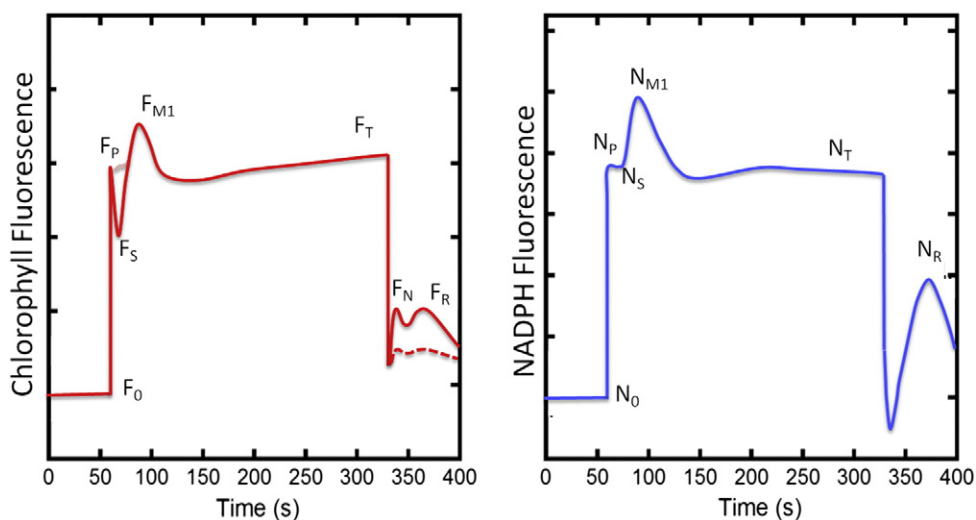


**Fig. 6.** Fluorescence transients in cyanobacteria. Left panel: Chlorophyll fluorescence Right panel: NADPH fluorescence. Designated points (discussed in the text) may be useful in assaying cellular metabolism.

increase in  $F_0$  was observed (Fig. 1C). The basis for this increase remains to be established, but it may reflect a hitherto unknown protective mechanism for dissipating excess excitation energy, albeit with the possibility of re-absorption. Likewise, an ostensibly photoprotective increase in photochemical quenching is observed upon reaching the  $C_i$ -limited state which we tentatively assign to the induction of flavodiiron proteins that dissipate photochemical electron [35,42–44] and have been shown to be induced under similar conditions as those studied here [18]. Upon termination of actinic light, chlorophyll and NADPH fluorescence quickly declines, although examination of the decays shows new kinetic features and decreased rates of oxidation as  $C_i$  becomes limiting. It is also observed that a small rise in chlorophyll fluorescence (here termed  $F_N$ ) occurring 5–10 s after actinic light termination and this feature is attributable to cyclic electron flow through NDH complexes ([46,49], See also Fig. 2 inset). This feature which is absent under some conditions, but enhanced in cells grown under  $C_i$  limitation likely due to the pool of reductant immediately available as reduced ferredoxin and NADPH. Later, a reduction event in chlorophyll and NADPH fluorescence is observed (here termed  $F_R$  and  $N_R$ ), attributed to the oxidation of sugars accumulated in the light and the attendant flow of reductant through the NADP and PQ pools to molecular oxygen consistent with the late (~30 s after actinic termination) and protracted kinetics of this feature.

Finally, the observed increase in the NADPH/NADP<sup>+</sup> ratio is consistent with recent findings regarding the mechanism of induction of the high affinity CCM via alterations in the activity of the transcriptional repressor, CcmR, caused by the interaction of NADP<sup>+</sup> and  $\alpha$ -KG [19]. The results are consistent with the previous finding that NADP<sup>+</sup> acts as an internal sensor of  $C_i$  status and inhibits induction of the CCM via its interaction with the transcriptional regulator CcmR. In those experiments, the induction of many genes occurred within 30 min of the onset of  $C_i$ -limitation, coinciding with the growth inflection and the pronounced changes in fluorescence kinetics observed here.

## Acknowledgments

The authors would like to thank Juliana Artier for her contributions towards developing the PAM fluorescence techniques employed in this study. This work was supported by the United States Department of Energy, Office of Basic Energy Sciences, DE-FG02-08ER15968.

## Appendix A. Supplementary data

Supplementary data to this article can be found online at <http://dx.doi.org/10.1016/j.bbabo.2014.12.001>.

## References

- [1] R.A. Berner, Atmospheric carbon dioxide levels over Phanerozoic time, *Science* 249 (1990) 1382–1386.
- [2] M.R. Badger, D. Hanson, G.D. Price, Evolution and diversity of CO<sub>2</sub> concentrating mechanisms in cyanobacteria, *Funct. Plant Biol.* 29 (2002) 161–173.
- [3] A.L. Johansson, S. Chakrabarty, C.L. Berthold, M. Hogbom, A. Warshel, P. Brzezinski, Proton-transport mechanisms in cytochrome c oxidase revealed by studies of kinetic isotope effects, *Biochim. Biophys. Acta* 1807 (2011) 1083–1094.
- [4] T. Ogawa, H. Mi, Cyanobacterial NADPH dehydrogenase complexes, *Photosynth. Res.* 93 (2007) 69–77.
- [5] G.D. Price, M.R. Badger, F.J. Woodger, B.M. Long, Advances in understanding the cyanobacterial CO<sub>2</sub>-concentrating-mechanism (CCM): functional components, C<sub>i</sub> transporters, diversity, genetic regulation and prospects for engineering into plants, *J. Exp. Bot.* 59 (2008) 1441–1461.
- [6] T.O. Yeates, C.A. Kerfeld, S. Heinhorst, G.C. Cannon, J.M. Shively, Protein-based organelles in bacteria: carboxysomes and related microcompartments, *Nat. Rev. Microbiol.* 6 (2008) 681–691.
- [7] A.G. Miller, B. Colman, Active transport and accumulation of bicarbonate by a unicellular cyanobacterium, *J. Bacteriol.* 143 (1980) 1253–1259.
- [8] A. Kaplan, M.R. Badger, J.A. Berry, Photosynthesis and intracellular inorganic carbon pool in the blue-green algae *Anabaena variabilis*: Response to external CO<sub>2</sub> concentration, *Planta* 149 (1980) 219–226.
- [9] G.D. Price, J.J.L. Pengelly, B. Forster, J. Du, S.M. Whitney, S. von Caemmerer, M.R. Badger, S.M. Howitt, J.R. Evans, The cyanobacterial CCM as a source of genes for improving photosynthetic CO<sub>2</sub> fixation in crop species, *J. Exp. Bot.* 64 (2013) 753–768.
- [10] A.P.M. Weber, A. Brautigam, The role of membrane transport in metabolic engineering of plant primary metabolism, *Curr. Opin. Biotechnol.* 24 (2013) 256–262.
- [11] M.R. Badger, A. Kaplan, J.A. Berry, Internal inorganic carbon pool of *Chlamydomonas reinhardtii*: evidence for a carbon dioxide-concentrating mechanism, *Plant Physiol.* 66 (1980) 407–413.
- [12] Y. Marcus, D. Zenvirth, E. Harel, A. Kaplan, Induction of HCO<sub>3</sub><sup>-</sup> transporting capability and high photosynthetic affinity to inorganic carbon by low concentration of CO<sub>2</sub> in *Anabaena variabilis*, *Plant Physiol.* 69 (1982) 1008–1012.
- [13] M. Shibata, H. Ohkawa, T. Kaneko, H. Fukuzawa, S. Tabata, A. Kaplan, T. Ogawa, Distinct constitutive and low-CO<sub>2</sub>-induced CO<sub>2</sub> uptake systems in cyanobacteria: genes involved and their phylogenetic relationship with homologous genes in other organisms, *Proc. Natl. Acad. Sci. U. S. A.* 98 (2001) 11789–11794.
- [14] B. Klughammer, D. Sultemeyer, M.R. Badger, G.D. Price, The involvement of NAD(P)H dehydrogenase subunits, NdhD3 and NdhF3, in high-affinity CO<sub>2</sub> uptake in *Synechococcus* sp. PCC7002 gives evidence for multiple NDH-1 complexes with specific roles in cyanobacteria, *Mol. Microbiol.* 32 (1999) 1305–1315.
- [15] R.G. Efremov, R. Baradaran, L.A. Sazanov, The architecture of respiratory complex I, *Nature* 465 (2010) 441–445.
- [16] N. Battchikova, M. Eisenhut, E.M. Aro, Cyanobacterial NDH-1 complexes: novel insights and remaining puzzles, *Biochim. Biophys. Acta* 1807 (2011) 935–944.



- [17] R.M. Figge, C. Cassier-Chauvat, F. Chauvat, R. Cerff, Characterization and analysis of an NAD(P)H dehydrogenase transcriptional regulator critical for the survival of cyanobacteria facing inorganic carbon starvation and osmotic stress, *Mol. Microbiol.* 39 (2001) 455–468.
- [18] H.L. Wang, B.L. Postier, R.L. Burnap, Alterations in global patterns of gene expression in *Synechocystis* sp. PCC 6803 in response to inorganic carbon limitation and the inactivation of *ndhR*, a LysR family regulator, *J. Biol. Chem.* 279 (2004) 5739–5751.
- [19] S.M. Daley, A.D. Kappell, M.J. Carrick, R.L. Burnap, Regulation of the cyanobacterial CO<sub>2</sub>-concentrating mechanism involves internal sensing of NADP<sup>+</sup> and alpha-ketoglutarate levels by transcription factor CcmR, *PLoS ONE* 7 (2012) e41286.
- [20] T. Nishimura, Y. Takahashi, O. Yamaguchi, H. Suzuki, S.I. Maeda, T. Omata, Mechanism of low CO<sub>2</sub>-induced activation of the *cmp* bicarbonate transporter operon by a LysR family protein in the cyanobacterium *Synechococcus elongatus* strain PCC 7942, *Mol. Microbiol.* 68 (2008) 98–109.
- [21] Y. Takahashi, O. Yamaguchi, T. Omata, Roles of CmpR, a LysR family transcriptional regulator, in acclimation of the cyanobacterium *Synechococcus* sp. strain PCC 7942 to low-CO<sub>2</sub> and high-light conditions, *Mol. Microbiol.* 52 (2004) 837–845.
- [22] F.J. Woodger, M.R. Badger, G.D. Price, Inorganic carbon limitation induces transcripts encoding components of the CO<sub>2</sub>-concentrating mechanism in *Synechococcus* sp. PCC7942 through a redox-independent pathway, *Plant Physiol.* 133 (2003) 2069–2080.
- [23] F.J. Woodger, M.R. Badger, G.D. Price, Sensing of inorganic carbon limitation in *Synechococcus* PCC7942 is correlated with the size of the internal inorganic carbon pool and involves oxygen, *Plant Physiol.* 139 (2005) 1959–1969.
- [24] P. Zhang, N. Battchikova, T. Jansen, J. Appel, T. Ogawa, E.M. Aro, Expression and functional roles of the two distinct NDH-1 complexes and the carbon acquisition complex NdhD3/NdhF3/CupA/Sil1735 in *Synechocystis* sp. PCC 6803, *Plant Cell* 16 (2004) 3326–3340.
- [25] M. Eisenhut, E.A. von Wobeser, L. Jonas, H. Schubert, B.W. Ibelings, H. Bauwe, H.C. Matthijs, M. Hagemann, Long-term response toward inorganic carbon limitation in wild type and glycolate turnover mutants of the cyanobacterium *Synechocystis* sp. strain PCC 6803, *Plant Physiol.* 144 (2007) 1946–1959.
- [26] J.W. Cooley, W.F. Vermaas, Succinate dehydrogenase and other respiratory pathways in thylakoid membranes of *Synechocystis* sp. strain PCC 6803: capacity comparisons and physiological function, *J. Bacteriol.* 183 (2001) 4251–4258.
- [27] G. Latouche, Z.G. Cerovic, F. Montagnini, I. Moya, Light-induced changes of NADPH fluorescence in isolated chloroplasts: a spectral and fluorescence lifetime study, *Biochim. Biophys. Acta Bioenerg.* 1460 (2000) 311–329.
- [28] Z. Cerovic, M. Bergher, Y. Goulas, S. Tosti, I. Moya, Simultaneous measurement of changes in red and blue fluorescence in illuminated isolated chloroplasts and leaf pieces: the contribution of NADPH to the blue fluorescence signal, *Photosynth. Res.* 36 (1993) 193–204.
- [29] H. Mi, C. Klughammer, U. Schreiber, Light-induced dynamic changes of NADPH fluorescence in *Synechocystis* PCC 6803 and its *ndhB*-defective mutant M55, *Plant Cell Physiol.* 41 (2000) 1129–1135.
- [30] U. Schreiber, C. Klughammer, New NADPH/9-AA module for the DUAL-PAM-100: description, operation and examples of application, PAM Application Notes, vol. 2, Heinz Walz GmbH, Effeltrich, Germany, 2009, pp. 1–13.
- [31] J. Kauny, P. Setif, NADPH fluorescence in the cyanobacterium *Synechocystis* sp. PCC 6803: a versatile probe for in vivo measurements of rates, yields and pools, *Biochim. Biophys. Acta* 1837 (2014) 792–801.
- [32] M.M. Allen, Simple conditions for growth of unicellular blue-green algae on plates, *J. Phycol.* 4 (1968) 1–4.
- [33] D. Campbell, V. Hurry, A.K. Clarke, P. Gustafsson, G. Oquist, Chlorophyll fluorescence analysis of cyanobacterial photosynthesis and acclimation, *Microbiol. Mol. Biol. Rev.* 62 (1998) 667–683.
- [34] R. Kaňa, E. Kotabová, O. Komárek, B. Šedivá, G.C. Papageorgiou, Govindjee, O. Prášil, The slow S to M fluorescence rise in cyanobacteria is due to a state 2 to state 1 transition, *Biochim. Biophys. Acta Bioenerg.* 1817 (2012) 1237–1247.
- [35] A.G. Miller, G.S. Espie, D. Bruce, Characterization of the non-photochemical quenching of chlorophyll fluorescence that occurs during the active accumulation of inorganic carbon in the cyanobacterium *Synechococcus* PCC 7942, *Photosynth. Res.* 49 (1996) 251–262.
- [36] A.G. Miller, G.S. Espie, D.T. Canvin, Chlorophyll-a fluorescence yield as a monitor of both active CO<sub>2</sub> and HCO<sub>3</sub><sup>-</sup> transport by the cyanobacterium *Synechococcus* UTEX 625, *Plant Physiol.* 86 (1988) 655–658.
- [37] M. Badger, U. Schreiber, Effects of inorganic carbon accumulation on photosynthetic oxygen reduction and cyclic electron flow in the cyanobacterium *Synechococcus* PCC7942, *Photosynth. Res.* 37 (1993) 177–191.
- [38] G.S. Espie, A.G. Miller, D.T. Canvin, High affinity transport of CO<sub>2</sub> in the cyanobacterium *Synechococcus* UTEX 625, *Plant Physiol.* 97 (1991) 943–953.
- [39] A.G. Miller, D.T. Canvin, Glycoaldehyde inhibits CO<sub>2</sub> fixation in the cyanobacterium *Synechococcus* UTEX-625 without inhibiting the accumulation of inorganic carbon or the associated quenching of chlorophyll a fluorescence, *Plant Physiol.* 91 (1989) 1044–1049.
- [40] D. Bruce, G. Samson, C. Carpenter, The origins of nonphotochemical quenching of chlorophyll fluorescence in photosynthesis. Direct quenching by P680+ in photosystem II enriched membranes at low pH, *Biochemistry* 36 (1997) 749–755.
- [41] G.D. Price, M.R. Badger, Ethoxymalate inhibition of CO<sub>2</sub> uptake in the cyanobacterium *Synechococcus* PCC7942 without Apparent Inhibition of Internal Carbonic Anhydrase Activity, *Plant Physiol.* 89 (1989) 37–43.
- [42] P. Zhang, M. Eisenhut, A.M. Brandt, D. Carmel, H.M. Silen, I. Vass, Y. Allahverdiyeva, T.A. Salminen, E.M. Aro, Operon flv4-flv2 provides cyanobacterial photosystem II with flexibility of electron transfer, *Plant Cell* 24 (2012) 1952–1971.
- [43] Y. Allahverdiyeva, H. Mustila, M. Ermakova, L. Bersanini, P. Richaud, G. Ajilani, N. Battchikova, L. Cournac, E.M. Aro, Flavodiiron proteins Flv1 and Flv3 enable cyanobacterial growth and photosynthesis under fluctuating light, *Proc. Natl. Acad. Sci. U. S. A.* 110 (2013) 4111–4116.
- [44] L. Bersanini, N. Battchikova, M. Jokel, A. Rehman, I. Vass, Y. Allahverdiyeva, E.-M. Aro, Flavodiiron protein Flv2/Flv4-related photoprotective mechanism dissipates excitation pressure of PSII in cooperation with phycobilisomes in cyanobacteria, *Plant Physiol.* 164 (2014) 805–818.
- [45] D. Kirilovsky, Photoprotection in cyanobacteria: the orange carotenoid protein (OCP)-related non-photochemical-quenching mechanism, *Photosynth. Res.* 93 (2007) 7–16.
- [46] N. Battchikova, L. Wei, L. Du, L. Bersanini, E.-M. Aro, W. Ma, Identification of novel Ssl0352 protein (Ndh5), essential for efficient operation of cyclic electron transport around photosystem I, in NADPH:plastoquinone oxidoreductase (NDH-1) complexes of *Synechocystis* sp. PCC 6803, *J. Biol. Chem.* 286 (2011) 36992–37001.
- [47] E. Gotoh, M. Matsumoto, Ogawa K.I., Y. Kobayashi, M. Tsuyama, A qualitative analysis of the regulation of cyclic electron flow around photosystem I from the post-illumination chlorophyll fluorescence transient in Arabidopsis: a new platform for the in vivo investigation of the chloroplast redox state, *Photosynth. Res.* 103 (2010) 111–123.
- [48] Y. Deng, J. Ye, H. Mi, Effects of low CO<sub>2</sub> on NAD(P)H dehydrogenase, a mediator of cyclic electron transport around photosystem I in the cyanobacterium *Synechocystis* PCC6803, *Plant Cell Physiol.* 44 (2003) 534–540.
- [49] D. Schwarz, H. Schubert, J. Georg, W.R. Hess, M. Hagemann, The gene sml0013 of *Synechocystis* species strain PCC 6803 encodes for a novel subunit of the NAD(P)H oxidoreductase or complex I that is ubiquitously distributed among Cyanobacteria, *Plant Physiol.* 163 (2013) 1191–1202.
- [50] Y.V. Bolyehvtseva, I.V. Terekhova, M. Roegner, N.V. Karapetyan, Effects of oxygen and photosynthesis carbon cycle reactions on kinetics of P700 redox transients in cyanobacterium *Arthrospira platensis* cells, *Biochem. Mosc.* 72 (2007) 275–281.
- [51] G. Bernat, J. Appel, T. Ogawa, M. Rogner, Distinct roles of multiple NDH-1 complexes in the cyanobacterial electron transport network as revealed by kinetic analysis of P700(+) reduction in various NDH-deficient mutants of *Synechocystis* sp. strain PCC6803, *J. Bacteriol.* 193 (2011) 292–295.
- [52] G. Renger, U. Schreiber, J. Amesz, D. Fork, Practical applications of fluorometric methods to algae and higher plant research, in: Govindjee (Ed.), Light emission by plants and bacteria, Academic Press, Orlando, USA, 1986, pp. 589–616.
- [53] M. Tamoi, T. Miyazaki, T. Fukamizo, S. Shigeoka, The Calvin cycle in cyanobacteria is regulated by CP12 via the NAD(H)/NADP(H) ratio under light/dark conditions, *Plant J.* 42 (2005) 504–513.
- [54] G. Papageorgiou, M. Tsimilli-Michael, K. Stamatakis, The fast and slow kinetics of chlorophyll a fluorescence induction in plants, algae and cyanobacteria: a viewpoint, *Photosynth. Res.* 94 (2007) 275–290.